Acta Biomaterialia 122 (2021) 186–198

Contents lists available at ScienceDirect

Acta Biomaterialia

journal homepage: www.elsevier.com/locate/actbio

Full length article

Biomimetic sulfated glycosaminoglycans maintain differentiation markers of breast epithelial cells and preferentially inhibit proliferation of cancer cells

Zeina Habli[a], Nataly Naser Al Deen[b], Waddah Malaeb[a], Nadine Mahfouz[b], Angela Mermerian[b], Rabih Talhouk[b,*], Rami Mhanna[a,*]

[a] Department of Biomedical Engineering, Maroun Semaan Faculty of Engineering and Architecture, American University of Beirut, Beirut, Beirut 1107 2020, Lebanon

[b] Department of Biology, Faculty of Arts and Sciences, American University of Beirut, Beirut, Beirut 1107 2020, Lebanon

ARTICLE INFO

Article history:
Received 28 August 2020
Revised 29 December 2020
Accepted 30 December 2020
Available online 11 January 2021

Keywords:
Glycosaminoglycans
Sulfated alginates
Biomimetics
Breast cancer
Therapeutics

ABSTRACT

Glycosaminoglycans (GAG) are key elements involved in various physiological and pathological processes including cancer. Several GAG-based drugs have been developed showing significant results and potential use as cancer therapeutics. We previously reported that alginate sulfate (AlgSulf), a GAG-mimetic, reduces the proliferation of lung adenocarcinoma cells. In this study, we evaluated the preferential effect of AlgSulf on tumorigenic and nontumorigenic mammary epithelial cells in 2D, 3D, and coculture conditions. AlgSulf were synthesized with different degrees of sulfation (DSs) varying from 0 to 2.7 and used at 100 μg/mL on HMT-3522 S1 (S1) nontumorigenic mammary epithelial cells and their tumorigenic counterparts HMT-3522 T4–2 (T4–2) cells. The anti-tumor properties of AlgSulf were assessed using trypan blue and bromodeoxyuridine proliferation (BrdU) assays, immunofluorescence staining and transwell invasion assay. Binding of insulin and epidermal growth factor (EGF) to sulfated substrates was measured using QCM-D and ELISA. In 2D, the cell growth rate of cells treated with AlgSulf was consistently lower compared to untreated controls ($p<0.001$) and surpassed the effect of the native GAG heparin (positive control). In 3D, AlgSulf preferentially hindered the growth rate and the invasion potential of tumorigenic T4–2 nodules while maintaining the formation of differentiated polarized nontumorigenic S1 acini. The preferential growth inhibition of tumorigenic cells by AlgSulf was confirmed in a coculture system ($p<0.001$). In the ELISA assay, a trend of EGF binding was detected for sulfated polysaccharides while QCM-D analysis showed negligible binding of insulin and EGF to sulfated substrates. The preferential effect mediated by the mimetic sulfated GAGs on cancer cells may in part be growth factor dependent. Our findings suggest a potential anticancer therapeutic role of AlgSulf for the development of anticancer drugs.

Statement of significance

Sulfated glycosaminoglycans (GAGs) of the extracellular matrix such as heparin interact with growth factors and growth factor receptors leading to profound effects on cellular processes including tumor growth and tumor inhibition. GAGs sulfation patterns have been shown to modulate their function through unclear mechanisms of action. Understanding the structure/activity relation in sulfated GAGs has led to the development of novel drugs for cancer treatment. Alginate sulfates (AlgSulf) are polysaccharides with defined homogenous sulfation codes mimicking native sulfated GAGs. Herein, we report a robust preferential inhibitory effect of the heparin-mimetic AlgSulf against breast cancer cells using a unique model of cell culture. Surprisingly, AlgSulf selectively targets cancer cells, rendering normal cells unaffected. Our findings suggest that AlgSulf represent a promising new class of anticancer biomimetic GAGs.

* Correspondence authors at: American University of Beirut P.O. Box 11-0236, Riad El Solh 1107 2020 Beirut, Lebanon.
E-mail addresses: rtalhouk@aub.edu.lb (R. Talhouk), rm136@aub.edu.lb (R. Mhanna).

https://doi.org/10.1016/j.actbio.2020.12.049
1742-7061/

1. Introduction

Breast cancer is the second most common cancer overall, and the fifth in causing death globally. It is the most prevalent type of malignancy in women worldwide in terms of incidence and mortality [1,2]. The breast tissue has a unique ability to evolve structurally during embryonic development, puberty, and pregnancy. These various stages of breast development and differentiation are regulated by the extracellular matrix (ECM), which is the guiding force that goes beyond providing architectural cell support. The ECM regulates multiple cellular behaviors such as proliferation, differentiation, and migration. In addition, it mediates cell-cell and cell-ECM communication, which when perturbed can lead to breast cancer (reviewed by [3]).

Glycosaminoglycans (GAGs) are key structural and functional elements of the ECM and are involved in a multitude of physiological and biological processes. They are large unbranched polysaccharide chains built by repeated disaccharide units with a variety of sulfation arrangements called "sulfation codes" [4]. Sulfated GAGs are synthesized in the Golgi apparatus and their sulfation patterns are regulated by sulfotransferases and endosulfatases [5]. The various sulfation patterns have been documented at multiple sites of the chains promoting high structural diversity and complexity. The latter enables GAGs to bind and regulate a formidable number of ligands, proteins, and growth factors (GF) involved in normal and cancer cell behaviors such as proliferation, differentiation, migration, and adhesion. Hence, GAGs are endowed with diverse biomedical functions that make these molecules very attractive for therapeutics.

The concept that GAGs can impact cancer progression has been investigated thoroughly during the past decades. So far, heparin (HN), a highly sulfated GAG, and HN species are the most therapeutically explored polysaccharides against cancer and their use has reached clinical settings. The frequent use of the anticoagulant HN, low molecular weight heparins (LMWH), and unfractionated heparin (UFH) in the treatment of cancer-associated thromboembolism has pointed out their antimetastatic activity reviewed in Grandoni et al. [6]. These HN species inhibit metastasis by blocking the interaction of platelets with tumor cells. The 6-O-sulfated glucosamine residue in HN molecules inhibits the binding of P- and L-selectin on platelets to their natural ligands on the surface of tumor cells. In the presence of HN species, cancer cells lose the protection conferred by platelets and become more susceptible to immune effector cells [7]. In addition, HN species inhibit the activity of the ECM enzyme heparanase and regulate the activity of mitogenic GF such as fibroblast growth factors (FGF) and vascular endothelial growth factors (VEGF), which in turn attenuate metastatic processes (reviewed in [8]). In addition, accumulating clinical evidence has shown that the administration of LMWH or UFH reduces mortality rates in cancer patients, possibly by angiogenesis reduction, metastasis inhibition, and the indirect pleiotropic actions on the coagulation system [9]. One drawback of using HN as a metastatic inhibitor is its anticoagulant property; the long-term use of these molecules could substantially lead to hemolysis and bleeding. Another downside is their structural diversity that can result in significant differences in the therapeutic dosage window, varying from one patient to another [10]. Other than HN and its analogues, modified heparan sulfate (HS) and chondroitin sulfate (CS), two sulfated natural GAGs in the ECM, have been shown to hold strong anticancer potential. For example, treatment with the HS mimetic KI-111 molecule [2-(4-fluoro-3-nitrobenzoyl)benzoic acetic anhydride] has been shown to inhibit sarcoma and cervical cancer cell adhesion, migration and growth *in vitro* [11]. On the other hand, treatment with carbodiimide-modified GAGs, neoHN, and neoCS, has been shown to reduce breast cancer and myeloma cell viability *in vitro* at low doses via apoptosis. Additionally, *in vivo* neoCS injections abolished breast cancer tumor growth in nude mice without causing damage to the adjacent normal tissue [12]. Another potent GAG is decorin which seems to be effective against metastatic breast cancer cells both *in vivo* and *in vitro* [13]. Although these molecules inhibit cancer proliferation, attachment, and distant metastatic seeding, their structural heterogeneity and size variability constitute a technical challenge in regard to insuring mass production with a consistent chemical composition.

The side effects associated with the anticancer activity of natural sulfated GAGs and the persistent technical challenges has hindered their therapeutic application and consequently encouraged the synthesis of synthetic heparins with precisely controlled structure [14] and sulfated biomimetics [15-17]. Alginates are biocompatible non-sulfated mimetic GAGs and are FDA-approved for use as a wound dressing material in humans [18,19]. Alginate sulfate (AlgSulf) has been shown to recognize and bind with high affinity to HN-binding GF, particularly basic fibroblast growth factor (FGF-2) [20,21], Insulin-like growth factor (IGF) [22] and nerve growth factor (NGF) [23]. In addition, studies have shown that AlgSulf induces stem cell chondrogenesis [21] and supports neurite growth in neuronal PC-12 cells and primary neurons [20,23]. Moreover, our group has recently shown that AlgSulf holds promising anticancer activity against lung adenocarcinoma (LUAD) [24]. This suggests that AlgSulf may have anticancer properties similar to HN against different types of solid tumors.

In the light of the promising potential of the HN-mimetic AlgSulf against cancer, we sought to evaluate its antitumorigenic potential against breast cancer using a unique three dimensional (3D) culture model of nontumorigenic and tumorigenic breast cells; nontumorigenic HMT-3522 S1 (S1) human mammary epithelial cells [25] and their tumorigenic counterparts HMT-3522 T4–2 (T4–2) cells [26]. The nontumorigenic mammary epithelial S1 cells form well-differentiated, growth-arrested, basoapically polarized structures, or acini, when cultured under 3D conditions. The central lumen within the S1 acini further indicates a close resemblance of the normal tissue architecture in the human breast. On the contrary, the tumorigenic counterparts T4–2 epithelial cells, derived from the HTM-3522 cancer progression series, form large and disorganized colonies or nodules, reminiscent of invasive breast cancer when cultured under 3D conditions. [27,28]. We investigated AlgSulf antiproliferative effects on cell growth rate in two dimension (2D) using bromodeoxyuridine (BrdU) and trypan blue exclusion assays. Then, we assessed AlgSulf effects on 3D cultured cells using immunofluorescence staining for diameter measurements, lumen assembly and localization of apicolateral polarity markers. We confirmed AlgSulf preferential inhibitory effects against cancer cells using a coculture model. We then examined its binding potential to GFs present in media supplements using quartz crystal microbalance with dissipation monitoring (QCM-D) analysis and enzyme-linked immunosorbent assay (ELISA). Our study provides support for the potential use of AlgSulf as a platform for breast cancer therapeutics.

2. Materials and methods

2.1. Preparation and characterization of sulfated alginates

AlgSulf were synthesized and characterized as described previously using SO_3 as a sulfation agent [21,29,30]. Briefly, alginate (Carl Roth GmbH + Co. KG, Molecular Weight (MW) ~ 160 kDa) were dissolved in water at 0.5% concentration and the DOWEX Marathon C ion exchanger was charged with an equal mass of tetrabutylammonium bromide. The charged resin was mixed with alginate solution at a ratio of 1:10 (w/v), stirred overnight, filtered, and then lyophilized. The produced alginate tetrabutylammonium salt was suspended in water-free DMF at 1% (w/v) containing a five-, seven- and nine-fold excess SO_3/pyridine per disaccharide unit to create AlgSulf$_n$ where n is the degree of sulfation (DS of 0.8, 2.0 and 2.7, respectively, and 0.0 for the native non-sulfated polysaccharides). The sulfur content was measured using an automatic elemental analyzer (CHNS-932, Leco, Germany) to measure the DS of the produced alginate sulfates. The DS denotes the average number of sulfate group per disaccharide repeating unit, it ranges between 0 (native alginate) and 4.0 (complete substitution of hydroxyl groups with sulfates). The IR spectra obtained in D_2O at 343 K using a Burker Advance 300 MHz spectrometer were consistent with literature of materials prepared by different procedures [22,31,32]. The MW of AlgSulf$_{2.0}$ and AlgSulf$_{2.7}$ are typically in the range of 220 kDa – 230 kDa while the MW of AlgSulf$_{0.8}$ is ~ 100 kDa. Heparin from porcine intestinal mucosa was used as a positive control, the material has most of its chains in the range of 17–19 kDa (as per the supplier) and a DS of 2.2 [33]. End-on biotinylation of alginates and heparin was performed via reductive amination. The end of the polysaccharide was reduced with biotin-LC-hydrazide followed by a reduction with $NaCNBH_3$. The synthesized molecule is denoted as b-AlgSulf$_n$ where b stands for biotinylation. For cell culture purposes, alginates were prepared at 1 mg/mL in serum-free DMEM/F12 (Lonza, Basel, Switzerland, BE12–719F) or serum-free RPMI (Lonza, Basel, Switzerland, BE12–115F) and filtered using syringe filters of 0.2 µm pore size (Corning, 431,229) and stored at 4 ºC for further use. Unless otherwise indicated, all reagents were obtained from Sigma Aldrich, St. Louis, MO, USA.

2.2. Cell culture

Nontumorigenic S1 HMT-3522 human mammary epithelial cells [25], between passages 52 and 60, were maintained as a monolayer (2D culture) in a chemically defined serum-free H14 medium at 37°C and 5% CO_2 in a humidified incubator. The tumorigenic counterparts of S1 cells, HMT-3522 T4–2 cells, were maintained under similar conditions but on tissue culture plastic coated with type-I collagen (BD Biosciences, Bedford, MA, USA, 354,236) in the absence of EGF [27,34]. S1 and T4–2 cells were propagated as previously described [28]. MDA-MB 231 epithelial breast cancer cells were cultured in RPMI supplemented with 10% fetal bovine serum (FBS) (Sigma, F-9665) and 1% penicillin/streptomycin (P/S) (Lonza, Basel, Switzerland, DE16–602E) at 37°C and 5% CO_2 in a humidified incubator. For 2D cultures, S1 and T4–2 cells were plated on plastic substrates at a density of 2.3 x 10^4 cells/cm^2 and 1.153 x 10^4 cells/cm^2, respectively. For 3D cultures, the drip method of cell culture was used to induce the formation of acini as previously described [35]. For S1 acini treatments, 100 µg/mL of AlgSulf$_n$ or HN was added pre-lumen formation on day 5 or post-lumen formation on day 9 till day 13 while T4–2 nodules were treated on day 3 till day 7. Cell culture media with treatment was replenished every 48 hrs throughout the culture period.

2.3. Trypan blue exclusion assay

S1 and T4–2 cells were plated in 6-well tissue culture plates in monolayers and treated at 40% confluence with 100 µg/mL of AlgSulf$_n$ or HN. MDA-MB 231 cells were plated in 12-well tissue culture plates in monolayers in serum-supplemented RPMI for 24 hrs. To prevent GAG saturation with random serum components at the sulfation sites, the serum-supplemented media was replaced with fresh media containing 1% FBS (serum-starved) after which the cells were treated at 40% confluence with 100 µg/mL of AlgSulf$_n$ or HN. At the corresponding time points, 24, 48 and 72 hrs post-treatment, cells were trypsinized and collected. Cells were then diluted in trypan blue (Sigma) at 1:1 ratio (vol/vol) and counted using a hemocytometer. Every experiment was ran in triplicate wells and counts for each well were repeated at least three times. Cell count was expressed as percentage growth with respect to control, untreated wells.

2.4. BrdU cell proliferation assay

S1, T4–2 and MDA-MB-231 cells were plated in 12-well tissue culture plates in monolayers and treated at 40% confluence with 100 µg/mL of AlgSulf$_n$ or HN for 72 hrs. To assess cell proliferation, cells were incubated with 25 µM bromodeoxyuridine (BrdU) (SIGMA) post-treatment for 18 hrs. After blocking and fixation, cells were treated with 2 N HCl, neutralized by borate buffer (0.1 M) and incubated with anti-BrdU primary antibody (Santa Cruz Biotechnology, Santa Cruz, CA) followed by CyTM3-conjugated secondary antibody (Jackson Immuno Research Laboratories, West Grove, PA). Stained cells were mounted with 4′6′-diamidino-2-phenylindole (DAPI, vector Laboratories, CA), placed under coverslips and visualized by immunofluorescence microscope (Zeiss). Positive cells were manually counted from at least 5 representative fields at 20x magnification and normalized to the total number of DAPI-positive cells.

2.5. Immunofluorescence staining

S1 and T4–2 plated in 4-well chamber slides (3D) were stained by immunofluorescence on days 13 and day 7, respectively, as described earlier [35]. Primary antibodies used were rabbit polyclonal against β-catenin (sc-7199, 1:100, Santa Cruz) and goat polyclonal against scrib (sc-11,049,1:100, Santa Cruz). Secondary antibodies conjugated with Alexa Fluor 488 (green) or Alexa Fluor 594 (red) (Invitrogen Molecular Probes, Eugene, OR) were used at the manufacturer's proposed dilutions (1:1000). The cells were examined and imaged with a laser scanning confocal microscope (Zeiss, LSM710).

2.6. Diameter measurements, lumen assembly and apicolateral polarity markers scoring

The fixed slides were examined with an upright fluorescent microscope (Leica, DF7000 T) using a 40x oil immersion objective to measure the diameter of acini/nodules cultured in 3D, assess lumen assembly, and score for the apicolateral distribution of β-catenin and scrib. A minimum of 120 S1 acini or T4–2 nodules were analyzed per group in each replicate. The size measurements and scoring were depicted from three independent replicates. The size of S1 acini and T4–2 nodules was measured manually by recording the diameter of each acinus or nodule using LAS X software. S1 acinar were grouped in two categories according to diameter size ($<$ 30 µm and $>$ 30 µm) while T4–2 nodules were grouped into three groups according to diameter size (30–50 µm, 50–100 µm and $>$ 100 µm). Lumen assembly was scored visually. In each condition, the stained slide was divided into 12 regions and the acini visualized by the ocular lens were assessed for having proper lumen assembly. Proper lumen assembly is depicted by a single layer of cells around a central lumen. This is done by focusing the 40x oil immersion objective in the z-axis up and down several times for each individual visualized acinus. Apicolateral distribution of β-catenin and scrib was scored visually in S1 acini having proper lumen assembly.

2.7. Transwell cell invasion assay

T4–2 cells were plated on cell culture inserts (Millipore, 8 µm pore size, PI8P01250) coated with 1:5 diluted Matrigel^{TM} (10 μL/cm2; BD Biosciences, 354,234) at a density of 75 x 103 cells per insert in DMEM:F-12 supplemented with 1% FBS. DMEM:F-12 supplemented with 10% FBS was added below the insert. Cells were incubated for 48 hrs then treated with 100 μg/mL of $AlgSulf_n$ or HN. The experiment was stopped 72 hrs post-treatment and inserts were processed as previously described [35].

2.8. Coculture of S1 with T4–2 tumor nodules

T4–2 cells transfected with pEGFP-N1 vector (GenBank Accession #U55762) to express GFP and fluoresce in green were used to be distinguished from S1 cells. S1 cells were plated in 6-well tissue culture plates and on day 6, EGF was withdrawn. GFP labeled T4–2 cells were cultured in 3D and incubated for 4 days. On the day of coculture (day 8 of S1 culture and day 4 of T4–2 cultured in 3D), T4–2 nodules were recovered from Matrigel™ using Dispase (BD Biosciences, 354,235) andwashed twice with DMEM/F12. Then, 50 μL of the recovered nodules were trypsinized with 50 μL of Trypsin 1X EDTA (Invitrogen Gibco, 25,200,056) for counting. The volume of T4–2 nodule suspension was adjusted to 1.6 x 10^4 cells/mL (around 2.4 x 10^4 cells per well) in H14 media without EGF. T4–2 nodules were then cocultured with S1 cells in 2D and incubated for 3 days before treatment. On day 3 of coculture, cells were treated with 100 μg/mL of $AlgSulf_n$ or HN, and treatments were replenished every other day till day 9. On the day of counting, the cocultured cells were trypsinized and counted using a hemocytometer. The number of fluorescent T4–2 cells were deducted from the total count of cells, the remaining cells were denoted as S1.

2.9. Build-up of $AlgSulf_n$ films and effect of sulfation on insulin and EGF binding using QCM-D

The build-up of $AlgSulf_n$ or HN films and subsequent insulin and EGF binding was assessed using QCM-D (Q-Sense E4, Gothenburg, Sweden). Biotinylation of gold-coated QCM-D crystals was performed as described previously [20,36]. Briefly, gold-coated QCM-D crystals were cleaned, dried with N_2 flow and irradiated with UV. The crystals were incubated overnight at room temperature in a 0.5 mM ethanolic solution of PEG thiol (99 mol%) and biotin PEG thiol (1 mol%) to form a self-assembled monolayer (SAM). The samples were mounted in the QCM-D flow cell and after signal stabilization, 25 μg/mL streptavidin (SA) was injected with a peristaltic pump for 10 min at a flow rate of 50 μL/min. Once the SA was well-deposited (portrayed in stable frequency and dissipation values), the films were washed with 1X PBS for 5 min followed by 5 min of no injection. After rinsing, b-$AlgSulf_n$ in 1X PBS (100 μg/mL) was injected using the same parameters as for SA. Finally, insulin (1 mg/mL) (Sigma, I9278–5ML) or EGF (30 μg/mL) (BD Biosciences, 354,001) was injected over the layered polysaccharide substrate at a flow rate of 50 μL/min and 25 μL/min, respectively, followed by no injection for 50 min. Overtones 1, 3, 5, and 7 were monitored, and the 3rd overtone was used for the assessment of the film's build-up.

2.10. Enzyme-linked immunosorbent assay (ELISA)

Murine EGF ABTS ELISA Development Kit (PeproTech, 900-K179) was used to prepare 96-well ELISA plates by incubating 100 μL of capture antibodies/well overnight according to the manufacturer's protocol. Wells were rinsed then incubated for 2 hrs with either (i) 100 μL EGF standard of varying concentrations (0, 15.6, 31.3, 62.5, 125, 250, 500, and 1000 pg/mL, to obtain the standard curve), (ii) 100 μL of EGF (DB Biosciences, 354,001) at a concentration of 300+/- pg/mL, (iii) 100 μL polysaccharides ($AlgSulf_n$ or HN) at varying concentrations (0.2, 0.02, or 0.002 μg/mL) , or (iv) by adding first 100 μL EGF (DB Biosciences, 354,001) at concentration of 300 +/- pg/ml and incubating for 2 hrs then adding 100 μL of $AlgSulf_n$ or HN at varying concentrations (0.2, 0.02, or 0.002 μg/ml) and incubating for another 2 hrs at room temperature. At the end of the incubation period, wells were rinsed and incubated with 100 μL detection antibody for 2 hrs at room temperature, rinsed, then incubated with 100 μL Avidin-HRP conjugate (1:2000) for 30 min at room temperature followed by 100 μL ABTS™ Peroxidase liquid substrate (ab14204) until color development (around 20 min). The optical density at 450 nm was recorded for the studied samples every 5 min for 15 min and corrected by subtracting readings at 540 nm (the presented results are from the 10 min recording). The reported results represent the concentration of EGF bound to the added molecules which were calculated by subtracting the absorbance measured in each sample from the absorbance measured in the control EGF (DB Biosciences, 354,001) sample (without polysaccharides). A standard curve was used to calculate the final concentration of EGF in each well.

2.11. Statistical analysis

Quantitative data were presented as means ± standard error of the mean (SEM) from three independent experiments. Statistical comparisons were done using SPSS version 23 software. Statistical evaluation was carried out by analysis of variance (ANOVA) followed by post-hoc Tukey's multiple comparison test. Significance levels were assigned by * for $p < 0.05$, ** for $p < 0.01$ and *** for $p < 0.001$. For immunofluorescence, when scoring was performed, two investigators analyzed the same slide. Independent cell cultures usually refer to different passages and batches.

3. Results

3.1. Alginate sulfates preferentially reduce tumorigenic breast cancer cell counts and proliferation when cultured in 2D monolayers

Nontumorigenic human breast epithelial S1 cells, their tumorigenic counterpart T4–2 cells and MDA-MB 231 breast cancer cells cultured in 2D conditions and treated with $AlgSulf_n$ (100 μg/mL) showed a decrease in cell count in all cell lines with increased DS of the biomimetic GAGs (Fig. 1 and supplementary figure S1). The effect was more evident in tumorigenic T4–2 cells and cancerous MDA-MB 231 ($p < 0.001$) compared to nontumorigenic S1 cells ($p < 0.01$). The cell count decreased upon treatment, while the number of dead cells was negligible and did not differ between the different treatment groups and controls. Treatment with $AlgSulf_{0.0}$ did not affect the cell growth rate in all cell lines; the cell counts were similar to untreated controls. However, treatment with AlgSulf resulted in reduced cell growth with a maximal reduction obtained for $AlgSulf_{2.0}$ treated cells. The effect of $AlgSulf_{2.0}$ treatment on cell growth rate was more potent on the tumorigenic T4–2 cells and the cancerous MDA-MB 231 cells (Figs. 1B and S1A) compared to nontumorigenic S1 cells (Fig. 1A). The cell count of S1 cells treated for 72 hrs was reduced by 21%, whereas that of T4–2 and MDA-MB 231 was reduced by 50% and 60%, respectively ($p < 0.001$). Similarly, treatment with the native GAG HN, positive control, did not affect S1 growth rate but reduced that of T4–2 cells and MDA-MB 231 cells significantly by 30% and 50%, respectively ($p < 0.05$).

Since trypan blue exclusion assay is not sufficiently sensitive for *in vitro* cytotoxicity testing and to confirm whether the reduction in viable cell counts induced by AlgSulf treatment was associated with reduction in proliferation, we performed BrdU incorporation assay. Consistent with the trypan blue exclusion assay results, AlgSulf treatment resulted in decreased BrdU incorporation into DNA in both T4–2 and MDA-MB 231 cells assessed 72 hrs

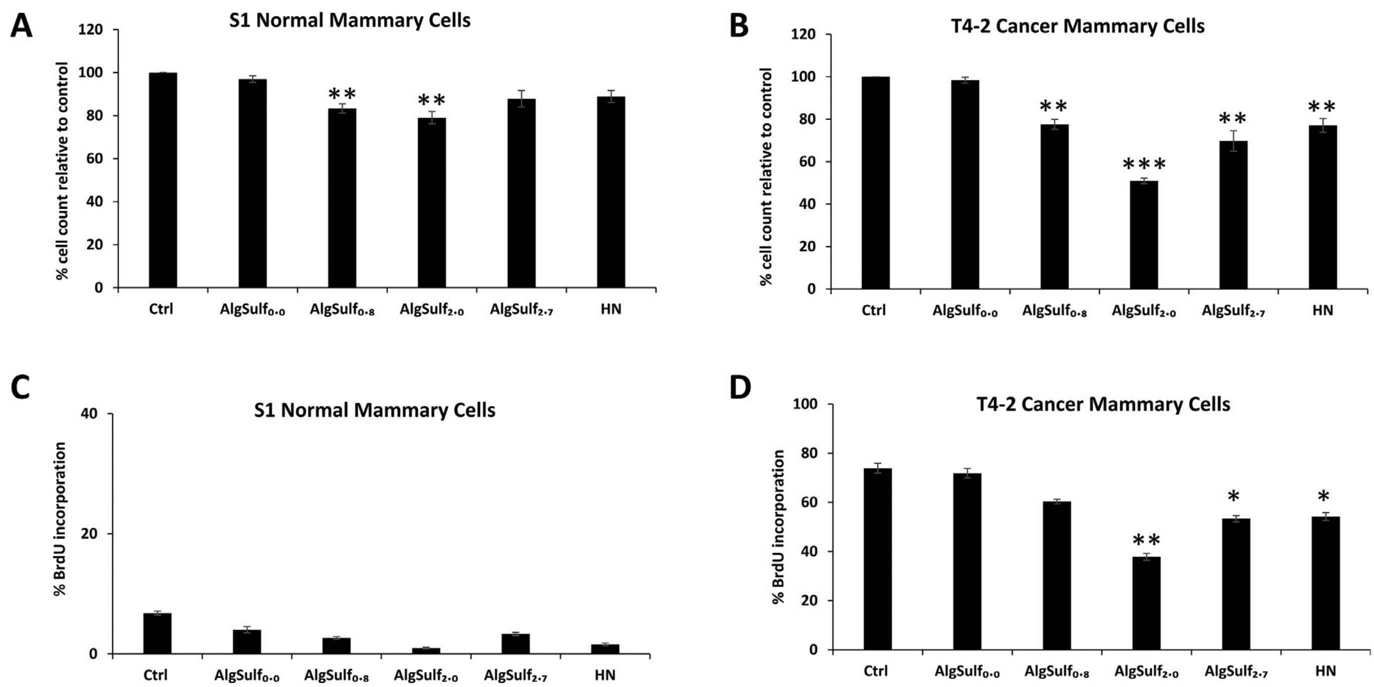

Fig. 1. Alginate Sulfate Preferentially Reduces Tumorigenic Breast Cancer Cell Counts and Proliferation in 2D Culture. S1 and T4–2 cells cultured under 2D conditions in 6-well plates and treated at 40% confluence with 100 μg/mL alginates of different DS, untreated cells were used as controls. **A, B)** S1 and T4–2 cell count was assessed using trypan blue exclusion assay at 72 hrs post treatment. The values depicted are the mean ±SEM from three separate experiments. **C, D)** S1 and T4–2 cell proliferation was assessed using BrdU cell proliferation assay at 72 hrs post treatment. The values depicted are the mean ±SEM from two separate experiments. *** denotes a p value < 0.001, ** denotes a p value < 0.01 and * denotes a p value < 0.05 compared to controls for each treatment using ANOVA followed by Post-hoc Tukey HSD test.

post treatment. The percentage of BrdU incorporation upon treatment was less than half in treated groups compared to untreated and $AlgSulf_{0.0}$ treated controls with $AlgSulf_{2.0}$ being the most potent (p<0.01) (Fig. 1D and supplementary figure S1B).

3.2. AlgSulf treatment of S1 3D cultures post-lumen assembly do not alter acinar structure nor β-catenin apical localization, but affect the latter when applied pre-lumen assembly

When cultured on Matrigel, S1 cells organize by day 7 in culture into acinar-like spheroids, approximately 30 μm in diameter, characterized by a single layer of cells around a central lumen with apicolateral polarity [28]. S1 cells treated on day 5 in culture (pre-lumen formation) with 100 μg/mL AlgSulf were assessed for acinar size, lumen assembly, and localization of polarity markers. Upon treatment, the percentage of acini with diameter > 30 μm significantly decreased compared to untreated and $AlgSulf_{0.0}$ treated control (Fig. 2A). Among the different DSs, $AlgSulf_{2.0}$ exhibited the highest effect on S1 acini, where the percentage of acini with diameter > 30 μm decreased significantly from 50% (control) to 36% (treated) ($p < 0.01$). A similar but less significant decrease was obtained with $AlgSulf_{2.7}$ ($p < 0.05$), while no significant decrease was observed with $AlgSulf_{0.8}$ or HN ($p > 0.05$). Lumen assembly was not altered in any of the treatment groups (Fig. 2B), but the localization of junctional markers was partially impaired. $AlgSulf_{2.0}$ significantly altered the distribution of β-catenin, a connexin 43 associated polarity protein [35,37]. β-catenin displayed a diffused localization compared to apicolateral localization, as seen in untreated and $AlgSulf_{0.0}$ treated controls. Only 50% of acini treated with $AlgSulf_{2.0}$ expressed apicolateral β-catenin compared to 71% of acini in untreated controls ($p < 0.05$) (Figs. 2C and 2D). Similarly, Scrib, a polarity marker, displayed a diffused localization in $AlgSulf_{2.0}$ treated cells (Fig. 2E).

To examine whether $AlgSulf_n$ affects the growth rate of S1 acini, and the localization of β-catenin post-lumen formation, S1 acini were treated on day 9 in culture with 100 μg/mL of $AlgSulf_n$. Upon treatment, the percentage of acini with diameter > 30 μm did not differ between treatment groups and controls (Fig. 3A). In addition, lumen assembly was not altered, nor apicolateral localization of β-catenin or Scrib was affected in any of the treatment groups. The percentage of acini with proper lumen formation was around 80% in all conditions (Fig. 3B), the percentage of acini with apicolateral distribution of β-catenin was around 60–65% in all conditions (Figs. 3C and 3D), and the percentage of acini with apicolateral distribution of Scrib was around 70–65% in untreated and $AlgSulf_{2.0}$ treated groups (Figure S2).

3.3. Alginate sulfates reduce growth rate of T4–2 tumorigenic mammary epithelial cells in 3D cultures and their invasion across reconstituted basement membrane

T4–2 cells develop structures reminiscent of invasive breast tumor nodules between 50 and 150 μm when cultured on reconstituted basement membrane matrix Matrigel [28,38]. When treated with AlgSulf, the percentage of T4–2 nodules with diameter > 100 μm decreased significantly compared to untreated and $AlgSulf_{0.0}$ treated controls, suggesting a reduced growth rate ($p < 0.001$) (Fig. 4A). $AlgSulf_{2.0}$ exerted the most potent effect on the growth of these tumorigenic cells; more than 80% of the nodules had a diameter size below 100 μm where most nodules fell in the small portion of the sizing spectrum as explained in the materials and methods (30 and 50 μm). Moreover, immunofluorescence of T4–2 nodules showed homogenous membrane distribution of both β-catenin and Scrib at cell-cell contacts (Fig. 4B). $AlgSulf_{2.0}$ did not affect the localization of β-catenin nor Scrib. Additionally, $AlgSulf_n$ not only affected the growth rate of tumorigenic cells but also reduced their invasion ability. In a transwell invasion assay where T4–2 cells are cultured in diluted Matrigel (1:5), $AlgSulf_n$ treatment decreased the number of invading cells with $AlgSulf_{2.0}$ being the most potent ($p < 0.01$) (Fig. 4C). $AlgSulf_{2.0}$ reduced the number of

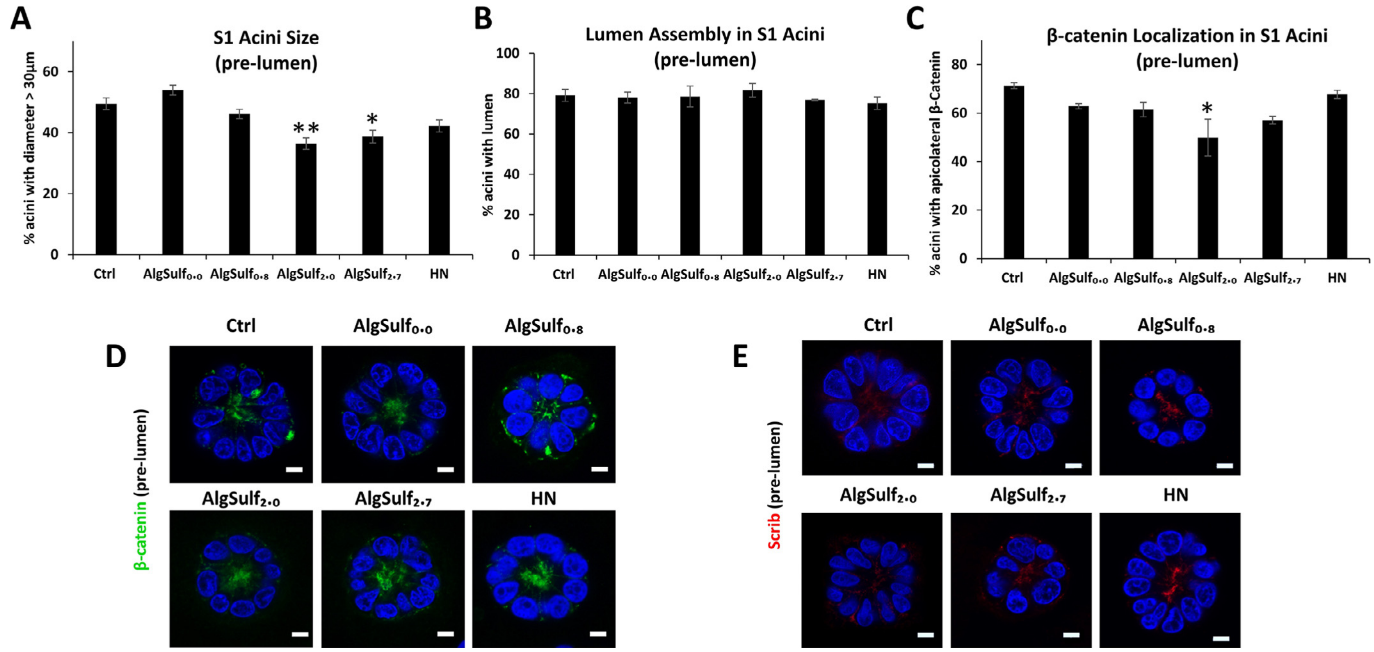

Fig. 2. Alginate Sulfate Reduces the Diameter of Acini and Alters Localization of β-catenin and Scrib in Nontumorigenic Mammary Acini when Treated Pre-Lumen Assembly. S1 cells were cultured in 3D conditions and treated with 100 µg/mL alginates of different DS on Day 5 (pre-lumen formation), untreated acini were used as controls. Bar graphs illustrate **A)** S1 acinar size distribution, **B)** percent acini with lumens **C)** percent of acini with apicolateral β-catenin. Size measurements and scoring were done from 12 different fields of each chamber containing 10 acinar each. The values depicted are the mean ±SEM from three separate experiments. Immuno-localization of **D)** β-catenin (green) and **F)** Scrib (red) are reported. Nuclei were counterstained with Hoechst (blue). Scale bar is 5 µm. *** denotes a p value < 0.001, ** denotes a p value < 0.01 and * denotes a p value < 0.05 compared to controls for each treatment using ANOVA followed by Post-hoc Tukey HSD test. (For interpretation of the references to colour in this figure legend, the reader is referred to the web version of this article.)

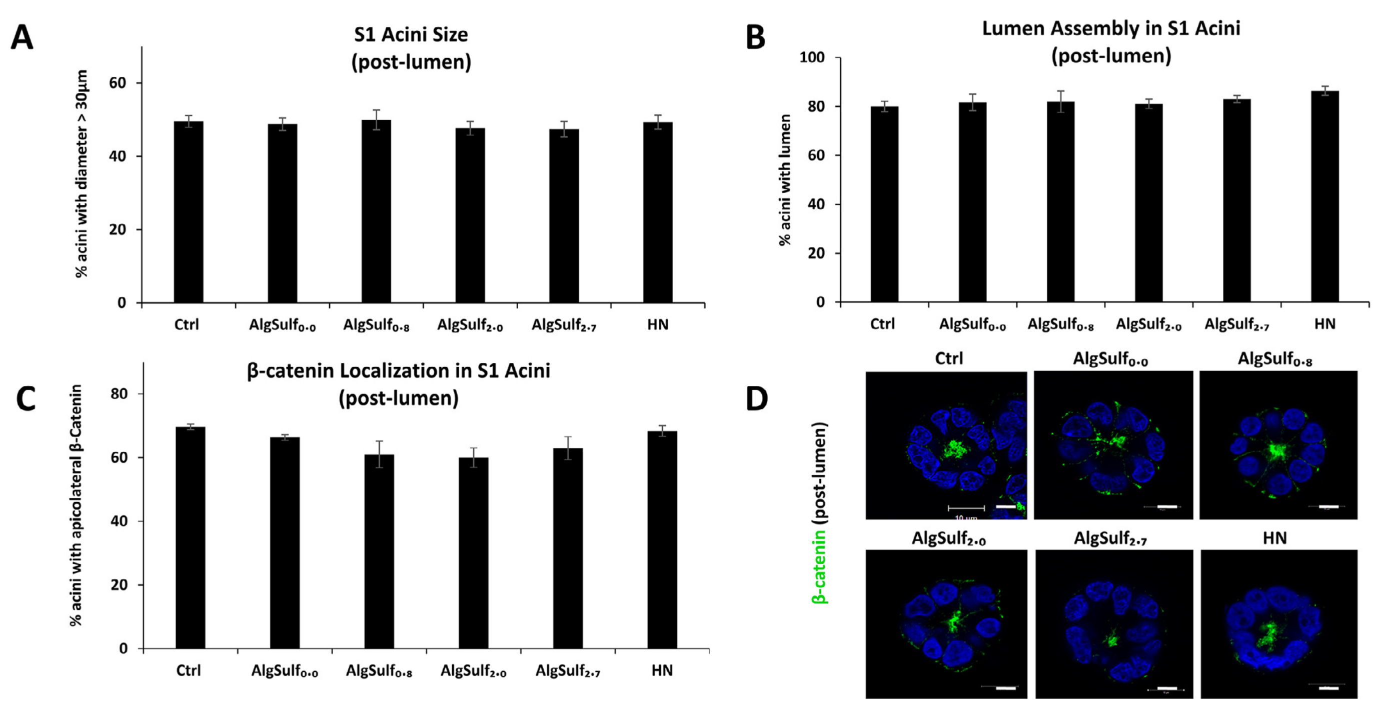

Fig. 3. Alginate Sulfate does not Affect Size, Lumen Assembly nor Localization of β-catenin in Nontumorigenic Mammary Epithelial Cells when Treated Post-Lumen Assembly. S1 cells were cultured in 3D conditions and treated with 100 µg/mL alginates of different DS on Day 9 (post-lumen formation), untreated acini were used as controls. Bar graphs illustrate **A)** S1 acinar size distribution, **B)** percent acini with lumens **C)** percent of acini with apicolateral β-catenin. Size measurements and scoring were done from 12 different fields of each chamber containing 10 acinar each. The values depicted are the mean ±SEM from three separate experiments. Immuno-localization of **D)** β-catenin (green) was reported and nuclei were counterstained with Hoechst (blue). Scale bar is 5 µm. *** denotes a p value < 0.001, ** denotes a p value < 0.01 and * denotes a p value < 0.05 compared to controls for each treatment using ANOVA followed by Post-hoc Tukey HSD test. (For interpretation of the references to colour in this figure legend, the reader is referred to the web version of this article.)

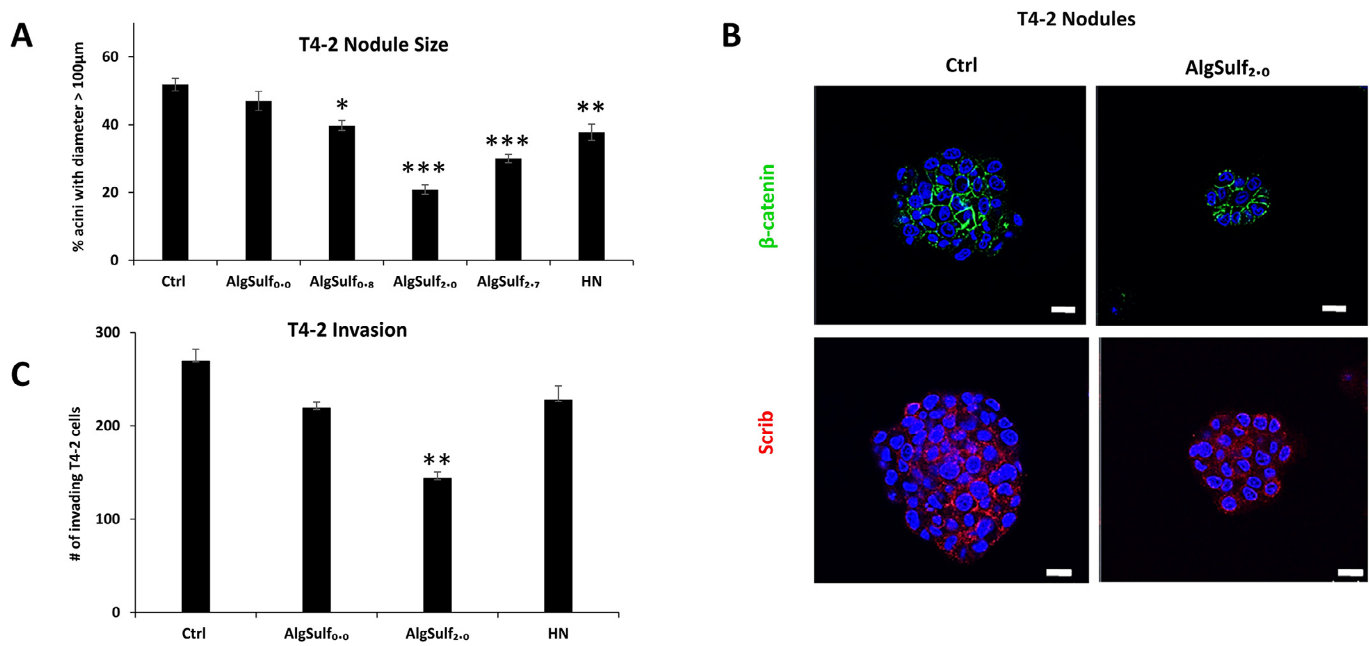

Fig. 4. Alginate Sulfate Significantly Reduces the Diameter of T4–2 Nodules and Invasion Capability. T4–2 cells were cultured in 3D conditions and treated with 100 µg/mL alginates with different DS on Day 3. The panels illustrate **A)** T4–2 diameter sizes measured from 12 different fields of the chamber containing 10 acinar each and **B)** the immuno-localization of β-catenin (green) and Scrib (red), and nuclei counterstained with Hoechst (blue). Scale bar is 20 µm. A bar graph illustrates **C)** percentage of invading T4–2 cells cultured in diluted Matrigel (1:5) and treated with 100 µg/mL alginates of different DS on Day 2. Invasion was assessed by transwell invasion assay; invading T4–2 cells were counted after fixation and Hoechst staining. The values depicted are the mean ±SEM from three separate experiments. *** denotes a p value < 0.001, ** denotes a p value < 0.01 and * denotes a p value < 0.05 compared to controls for each treatment using ANOVA and Post-hoc Tukey HSD test. (For interpretation of the references to colour in this figure legend, the reader is referred to the web version of this article.)

invading cells almost to half while no significant decrease was obtained with HN nor with AlgSulf$_{0.0}$.

3.4. Alginate sulfates preferentially reduce mammary epithelial tumor cell growth rate in a coculture system

To reproduce the mammary tumor microenvironment *in vitro*, where tumorigenic cells grow in close proximity to nontumorigenic cells, a coculture system was used [38]. Coculture systems are comprised of two cell types combined to recreate the tumor microenvironment milieu. In our case, T4–2 small nodules were cultured on nonpolarized monolayered S1 nontumorigenic cells as previously described [39]. Upon treatment, AlgSulf$_{2.0}$ significantly reduced the cell count of GFP-labelled T4–2 cells without affecting that of S1 cells ($p < 0.001$) (Fig. 5). AlgSulf$_{2.0}$ reduced the growth rate of T4–2 nodules up to 38% compared to untreated, AlgSulf$_{0.0}$, and HN treated controls. On the other hand, the growth rate of S1 cell count was not affected; it was maintained in all conditions (Fig. 5A and 5B).

3.5. Alginate sulfates revert the malignant phenotype of tumorigenic mammary epithelial cells

Tumorigenic T4–2 cells can be induced to form architecturally normal acinus-like structures in 3D conditions when subjected to microenvironmental signaling modifications or transient mechanical compressive forces [40-43]. As mentioned previously, T4–2 cells form disorganized colonies of cells when cultured in Matrigel. The majority of acini had a diameter size > 100 µm, and the smallest ones, although very rare, had a diameter size of around 30 µm (Fig. 6A). Treatment with AlgSulf$_{2.0}$ induced the formation of reverted structures most similar to S1 acini in terms of size, lumen assembly, and polarity (Fig. 6B). The acini-like structures formed by the reverted T4–2 cells had a hollow lumen similar to S1 acini. β-catenin was redistributed from a disorganized pattern in control T4–2 nodules to an apicolateral pattern in each spheroid, closely resembling β-catenin localization in untreated S1 acini. The size of reverted T4–2 acini was almost similar to S1 acini ranging between 30 and 45 µm in diameter. Scoring for reversion (lumen assembly and β-catenin apicolateral distribution) showed that around 60 nodules per chamber area (~1.7 cm^2), albeit a minor percentage of total cell population, reverted from malignant phenotype to normal phenotype. The reversion was not recorded in the untreated controls (Fig. 6C).

3.6. Alginate sulfates may regulate cell growth through growth factor binding

GAGs are either components of the ECM, located on cell surfaces, or found in small secretory vesicles in some cell types. They bind to soluble mediators such as GF and cytokines, and modulate cell signaling and proliferation. Through binding, GAGs modulate the mediators' bioactivity and bioavailability for a long period according to the cell's need [44,45]. Two approaches were used to test the binding affinity of AlgSulf to insulin and EGF, two essential media supplements in the S1/T4–2 culture system. The first platform used is the QCM-D analysis, where polysaccharides (AlgSulf$_n$ and HN), resembling GAGs anchored to cell surfaces, were assessed for their ability to bind insulin and EGF. The second platform is ELISA, in which the GAGs are used in solution, simulating polysaccharides present in the vicinity of the cells, as the case in our culture model. QCM-D results showed that neither insulin nor EGF binds to the immobilized sulfated polysaccharides (Figs. 7A and 7B). As shown in the figures, the adsorption of SA (streptavidin) then AlgSulf$_n$ lead to a shift in frequency and dissipation in all substrates. As the DS increased, the frequency shifts increased simultaneously as follows: b-AlgSulf$_{0.0}$ < *b*-AlgSulf$_{0.8}$ < *b*-AlgSulf$_{2.0}$. Upon adding insulin or EGF, the frequency and dissipation curves remained unaffected, indicating that both GFs do not adsorb to the sulfated polysaccharides layer. Several concentra-

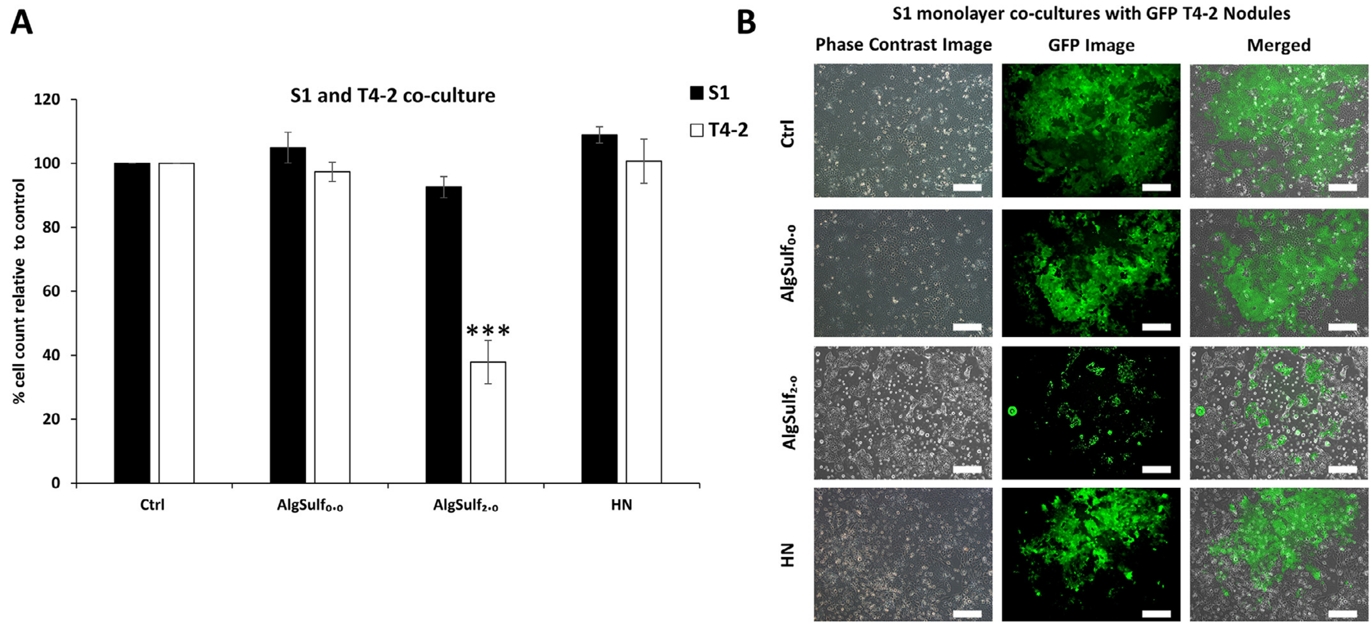

Fig. 5. Alginate Sulfate Preferentially Reduces Tumorigenic Mammary Epithelial Cell Count in a Coculture System. Sub-confluent S1 cells were cocultured with GFP-labeled T4–2 nodules and treated with 100 μg/mL of AlgSulf$_{0.0}$, AlgSulf$_{2.0}$ or HN, untreated cocultured cells were used as controls. The bar graph shows **A)** S1 and T4–2 cell counts as assessed under bright field and fluorescence. **B)** Representative images from coculture shows S1 cells (phase-contract) and T4–2 cells (in green fluorescence) at 10X magnification. Scale bar is 500 μm. (For interpretation of the references to colour in this figure legend, the reader is referred to the web version of this article.)

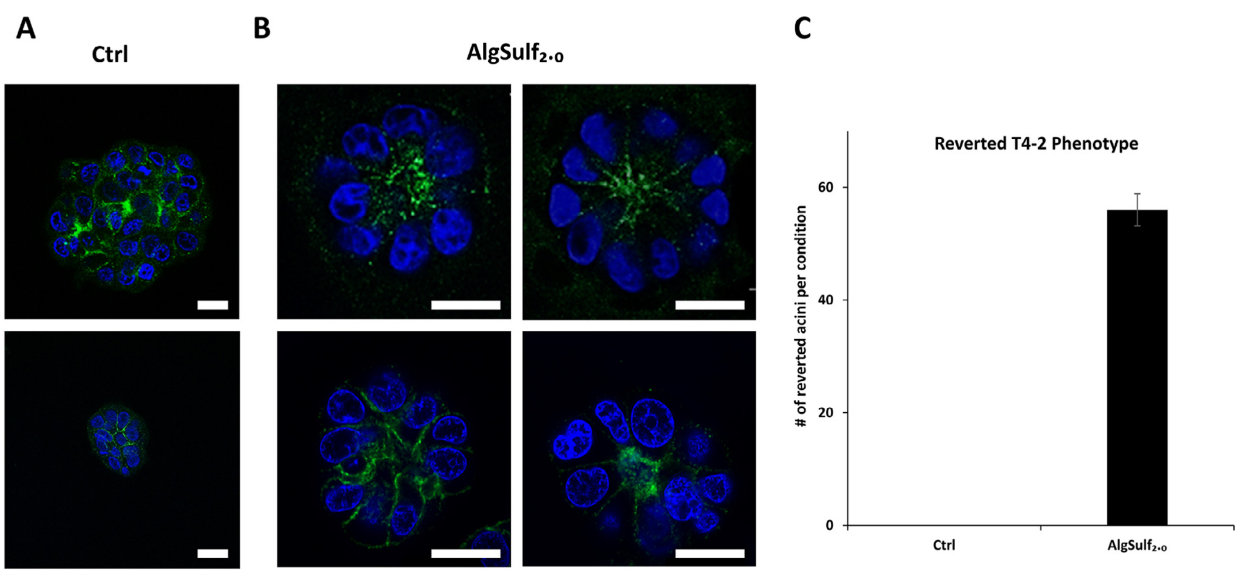

Fig. 6. Alginate Sulfate Restores Cell Polarization and Lumen Assembly Capacity in Tumorigenic Mammary Epithelial Cells. T4–2 cells were cultured in 3D conditions and treated with 100 μg/mL AlgSulf$_{2.0}$ on Day 3. T4–2 nodules were stained with β-catenin (green) and nuclei were counterstained with Hoechst (blue). Immuno-localization of β-catenin illustrates **A)** untreated T4–2 nodules (scale bar is 20 μm) and **B)** treated T4–2 nodules showing reversion to a nontumorigenic phenotype (scale bar is 20 μm). **C)** T4–2 reverted phenotype was scored by proper lumen assembly and apicolateral distribution of β-catenin from 12 different fields of the chamber containing 10 acinar each. The values depicted are the mean ±SEM from three separate experiments. (For interpretation of the references to colour in this figure legend, the reader is referred to the web version of this article.)

tions of insulin, EGF, and sulfated polysaccharides were used in the build-up layering, and all showed no frequency shift upon adding the media supplements, unlike FGF-2 and NGF that show a significant increase in binding upon increased sulfation [20,21,23]. On the contrary, ELISA results showed a pattern of EGF binding upon treatment with varying concentrations of AlgSulf$_{0.0}$, AlgSulf$_{2.0,}$ and HN in solution. As shown in Fig. 7C, EGF binds to AlgSulf$_{2.0}$ and HN more so than to AlgSulf$_{0.0}$. Upon mixing 300 +/- pg/mL EGF with 0.002 μg/mL polysaccharides, HN bound to 153 pg/mL, AlgSulf$_{2.0}$ bound to 100 pg/mL whereas AlgSulf$_{0.0}$ bound to 53 pg/mL. Despite the clear trend of polysaccharides binding to EGF, the binding was not statistically significant ($p = = 0.069$). The observed trend in EGF binding to AlgSulf$_{2.0}$ and HN as well as our previous studies showing significant binding of AlgSulf$_{2.0}$ to HN-binding GFs [20-23], indicate that sulfation-dependent growth factor binding may modulate the growth rate of S1 and T4–2 cells.

4. Discussion

The ECM mediates a wealth of signals that dictate cells' fate. GAGs of the ECM play a pivotal role in a multitude of physiological processes and are heavily involved in all the pathophysiologi-

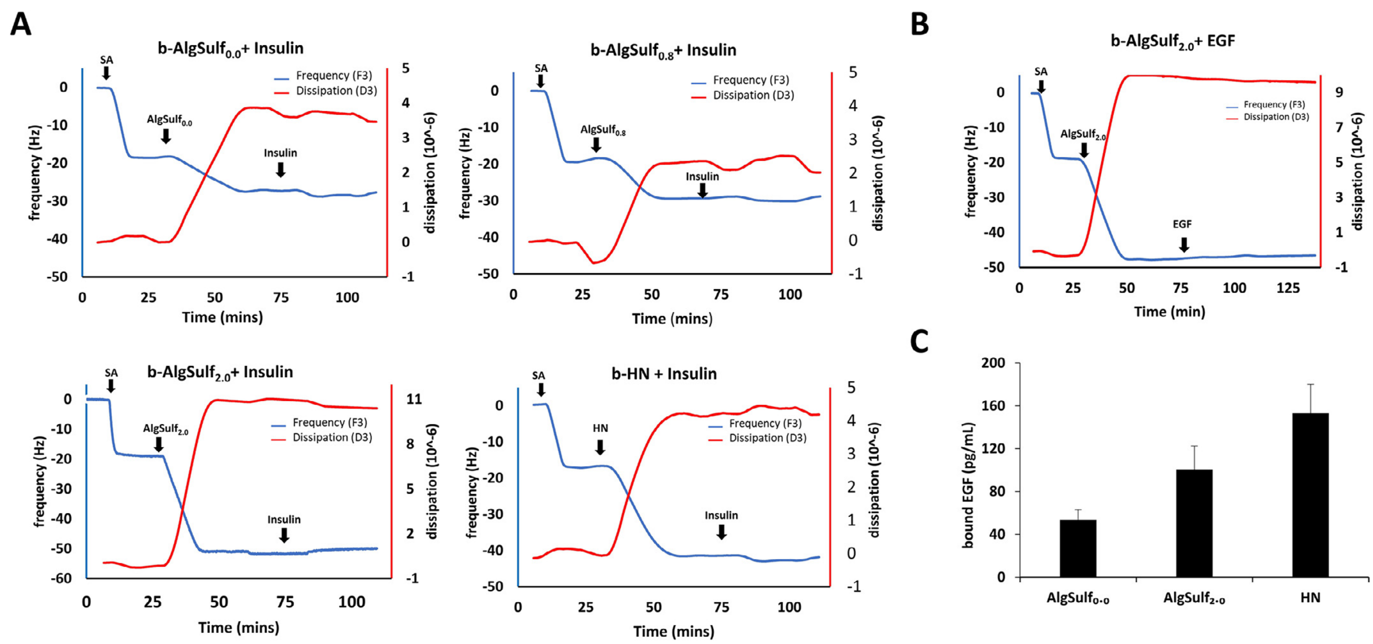

Fig. 7. Alginate Sulfate Does not Act as a Sink for Insulin and EGF. Graphs showing **A)** normalized resonance frequency shift and dissipation shift of the 15 MHz detection frequency for the buildup of b-AlgSulf$_{0.0}$, b-AlgSulf$_{2.0}$ or b-HN, and adsorption of insulin to the films, **B)** normalized resonance frequency shift and dissipation shift for the build-up of b-AlgSulf$_{2.0}$ and EGF adsorption and **C)** Quantitative assessment of EGF binding to 0.002 µg/mL AlgSulf$_{0.0}$, AlgSulf$_{2.0}$ or HN (used as a positive control) in solution by ELISA. Absorbance was normalized by relative quantitation of the absorbance value at 450 nm. Each value is the mean ±SEM of three separate experiments.

cal stages of cancer progression [44]. Modifications in the sulfation codes of GAGs are tied to mammary development, mammary cancer and associated anticancer therapies [46-48]. Interestingly, several studies have shown that sulfated GAGs such as HN, HS, CS and decorin possess antiproliferative and anti-metastatic activity against tumorigenic cells in *in vivo* and *in vitro* models 9,11,13,49]. AlgSulf, a biomimetic sulfated GAG, possesses HN-mimetic anticoagulant, anti-inflammatory, and GF binding properties that are tied to the polysaccharide DS [22,31,50,51]. We recently reported the antitumor activity of AlgSulf on LUAD *in vitro* [24]; however, its role against breast cancer development and mechanisms of action are still lacking.

4.1. AlgSulf reduce proliferation of mammary epithelial cells

Our results uncover a preferential antitumorigenic potential of AlgSulf on breast cancer cells using 3D and coculture models. Unlike non-sulfated GAGs which have shown to increase cell proliferation in some cases [48,52], we provide evidence that our mimetic sulfated GAGs preferentially reduce the viable cell count and proliferation of T4–2 and MDA-MB-231 breast cancer cells while marginally affecting that of nontumorigenic S1 cells in 2D cultures. The uptake of BrdU by the S1 nontumorigenic mammary cells was very limited even in the control condition (Fig. 1C). This could be attributed to the fact that the S1 cells are inherently slow proliferating cells and were treated with BrdU on day 8 during their quiescence phase even at sub-confluent densities [28]. This observation is in line with our recent study by Al Matari et al. where AlgSulf exhibited potent antiproliferative activity on human H1792 and murine MDA-F471 LUAD cells in 2D cultures without affecting the growth rate of RWPE1 normal prostate cells [24]. In support of our finding, several studies have shown that sulfated GAG-based therapies target cancer cells without affecting normal cells. For instance, novel neoglycan molecules (modified CS with carbodiimide) reduce mammary cell viability *in vitro* and abolish tumor growth in immunocompromised mice without affecting the surrounding normal tissue [12]. Additionally, xyloside 2-(6-hydroxynaphthyl) β-D-xylopyranoside (XylNapOH), a primer for GAG synthesis, selectively inhibits the proliferation of T264 bladder and HCC70 breast carcinoma cells in 2D cultures without causing growth retardation in HFL-1 human embryonic fibroblast cells [53]. However, unlike 3D cultures, 2D cultures do not accurately recapitulate the human tissue architecture *in vitro* and thus may respond differently to treatment [54].

4.2. Quiescent mammary epithelial cells in 3D cultures are insensitive to AlgSulf

3D cultures of nontumorigenic breast epithelial cells, which restore many aspects of the human breast tissue architecture, are better indicators for drug efficacy. The 3D culture model serves to distinguish between tumorigenic and nontumorigenic cells, and offers striking proliferative and morphological differential responses to anticancer drugs in comparison to 2D culture models [55,56]. Nontumorigenic S1 cells form polarized growth-arrested acini that are reminiscent of the breast acinus *in vivo,* while tumorigenic T4–2 cells, derived from the HTM-3522 cancer progression series, form disorganized continuously proliferating nodules [28].

Treating S1 acini late in culture in their quiescent and fully functional state does not affect the apicolateral axis that is well established where β-catenin and scrib are maintained in apicolateral localization. These two proteins have key roles in regulating different aspects of epithelial growth such as proliferation, apoptosis, differentiation, and tissue organization [57]. In line with a previous study, we have shown that treating differentiated S1 acini with 18α-Glycyrrhetinic acid (18α-GA), a gap junction inhibitor, does not affect their *in vivo* like morphology [37]. However, when treating S1 acini during their proliferation phase, S1 cells maintain the ability to assemble around a lumen but their apicolateral polarity is partially disrupted. In addition, their proliferation rate decreases as the acini maintain a smaller size. Indeed, mammary epithelial cells with disrupted apicolateral polarity exhibit enhanced cell cycle entry but their proliferation rate is not boosted [58,59]. For example, non-neoplastic mammary epithelial MCF10 cells depleted from scrib failed to polarize and migrate, but their proliferation was not affected [60]. Notably, the nonattainment of polarity obtained in our 3D cultures seems to sensitize S1 acini to AlgSulf. This induced-growth reduction suggests that the targeted activity of AlgSulf seems to be blocking the entry of cells into the cell cycle instead of inducing cell death because apicolateral polarity is impaired with non-enhanced proliferation. Furthermore, the nonattainment of polarity axis suggests that AlgSulf may modulate polarity likely through tight or gap junctions-related signaling pathways such as the Wnt/β-catenin pathway previously observed with several sulfated GAGs. For example, syndecans, type I transmembrane HS proteoglycans, dysregulate some components of theWnt signaling pathways. The overexpression of syndecan-4 in multiple mammalian cells inhibited the Wnt/β-catenin pathway [61]. Also, treatment with exogenous highly sulfated CS-E (chondroitin sulfate-E) negatively regulated the Wnt/β-catenin pathway of murine mammary carcinoma cells in 3D cultures [62]. In fact, we have shown previously that the mislocalization of β-catenin and Scrib from apicolateral domains of the S1 acini is associated with loss of apical polarity [35].

4.3. Tumorigenic mammary epithelial cells in 3D cultures are sensitive to AlgSulf

We further investigated the antiproliferative potential of the biomimetic sulfated GAGs on the growth rate and invasion of the tumorigenic T4–2 cells cultured on Matrigel. Our results demonstrate that AlgSulf possesses a preferential antiproliferative and anti-invasive effect against tumorigenic cells. Al Matari et al. reported that AlgSulf has significant antiproliferative effects that are time- and dose-dependent on LUAD cancer stem cells propagated in 3D conditions using the sphere-forming assay. In addition, AlgSulf inhibited the migratory abilities of LUAD cells in 2D conditions using the wound healing/scratch assay [24]. Similarly, CS-E inhibited the invasive protrusion formation of murine mammary carcinoma EMT6 spheroids and decreased their motility and migratory abilities. CS-E-treatment targeted the pro-metastatic ECM *Col1a1* gene and downregulated the pro-tumorigenic Wnt/β-catenin pathway [62]. Moreover, AlgSulf induced a marked increase in the number of T4–2 cellular aggregates with reversed phenotype. T4–2 cells can form growth-arrested multicellular aggregates having hallmarks of the mammary organization upon inhibition of the EGFR and β1-integrin pathways [40-42]. The observed reversion of tumorigenic cells upon treatment advocates that AlgSulf can also partially reverse the tumorigenic phenotype that T4–2 cells acquire on Matrigel and partially restore their apicolateral polarity axis and assembly around a lumen.

Although *in vivo* experiments were not implemented in this work, the HMT-3522 breast tumor progression series recapitulates the histological characteristics of human breast carcinoma, specifically the ductal carcinoma *in situ* (DCIS), when grown in 3D conditions [63]. This cell model encompasses the spectrum of tumor development and recapitulates the *in vivo* characteristics. As such, it has been thoroughly studied and adopted in screening for novel treatments and targets in breast cancer in many studies (reviewed in [64]). Unlike T4–2 cells, under 3D conditions, MDA-MB 231 cells can either form disorganized stellate nodules with poor cell-cell adhesion and elongated cell bodies with invasive processes when grown on Matrigel [65,66] or spheroid structures when grown on agarose gel [67]. These 3D structures do not recapitulate the different stages of breast cancer progression nor simulate the complexity of the different types of breast cancer. In addition, these cells do not have a normal counterpart with the same genetic lineage. Therefore, MDA-MB 231 use was exclusive to 2D culture conditions to highlight the promising antiproliferative effects of AlgSulf against these aggressive, metastatic, and invasive mammary tumor cells.

4.4. Cocultures have better resemblance to study AlgSulf effects

Although 3D culture systems of nontumorigenic breast cells restore many features of the tissue architecture, coculture systems, while very rarely used, give a better resemblance to the tumor microenvironment where there is close contact between nontumorigenic and tumorigenic cells [38]. The used coculture setup restores to some extent the breast cancer tissue architecture in which the tumorigenic T4–2 mammary cells develop into 3D growth patterns over the nontumorigenic S1 mammary epithelial cell bed as previously described by Vidi et al. [39]. AlgSulf selectively targeted the GFP-labeled T4–2 cells in coculture without altering the growth rate of the nontumorigenic S1 cells, supporting the selective antitumorigenic activity of AlgSulf. To the best of our knowledge, such preferential activity in a coculture system has not been previously recorded with sulfated GAGs. For instance, XylNapOH treatment inhibited the proliferation of both matched normal HFL-1 and cancer T24 mammary cells in a coculture model although it selectively reduced the proliferation of T24 cells but not HFL-1 cells when grown separately in 2D culture [53].

Noteworthy is the significant antiproliferative effects observed with AlgSulf$_{2.0}$ on mammary cancer cells in 2D, 3D and coculture conditions compared to other AlgSulf or HN. While we have no solid explanation of why intermediate DS exhibited the most potent effects, which is in agreement with previous findings [68,69] and our previous studies [20,24], we believe that this intermediate DS exists because it provides better matching and consequently higher affinity to binding sites on the affected GFs or binding partners. When the sulfated polysaccharides bind to substrates, the brushes formed with DS=2.7 are stiffer than the lower sulfation and structurally less flexible to enable AlgSulf interaction with growth modulators and GFs. This makes the intermediate DS more effective in solution or bound to substrates in targeting the proliferation of cancer cells. The current study does not control for the effect that might exist due to the regioselective distribution of sulfate groups on the backbone of the alginates. Determining the exact sulfation distribution is challenging for alginates which carry 4 secondary OH groups and exhibit very broad NMR signals in part due to their high MW. While we use the same alginate source to create the different sulfated polysaccharides, the sulfation process and the introduced sulfate groups contribute to the MW and thus sulfated products do not have the same MWs. The MW of herein used raw alginates (~160 kDa) when sulfated for a product of DS~2, would theoretically increase by ~37 kDa, resulting in a polysaccharide of ~200 kDa. Considering a MW measurement error of approximately 10%, makes us believe that the attained MW for AlgSulf$_{2.0}$ and AlgSulf$_{2.7}$ (220 – 230 kDa) are within an explainable range. Interestingly, alginates with a DS~0.8, had a MW in the range of 100 kDa, which might be caused by hydrolysis of the starting material or differential interaction with the GPC column. It might be that such a hydrolysis is not permitted in the presence of a high concentration of the sulfation agent. While the low sulfation alginates exhibit a lower MW than expected, the trends are consistent with those obtained earlier for the sulfation of hyaluronic acid where a low sulfation polymer (DS=1) had a lower MW than those with a higher sulfation (DS=2.7) [33]. Moreover, HN used in the current study as a positive control has a different molecular composition and a lower MW. The MW of sulfated polysaccharides has been shown to modulate transforming growth factor $\beta-1$ (TGF-β1) binding, where a lower MW was associated with higher binding of TGF-β1 for molecules of the same DS [33]. However, we have seen in our previous studies that FGF-2 binds to HN less than sulfated alginates even for sulfated alginates with lower DS (DS=0.8). We also observe here that the effects of HN on EGF binding and cell proliferation, albeit less pronounced, are not drastically different from $AlgSulf_{2.0}$ (similar DS). This suggests that the DS and its distribution has a more pronounced role on growth factor binding and other biological responses than MW in the ranges used in the above-mentioned studies. These findings strongly incentivize systematic investigations on the role of sulfated polysaccharides MWs including large MW polysaccharides such as alginate and hyaluronan where steric hindrance becomes more important.

4.5. AlgSulf binding to media-supplemented growth inducing factors

GAGs are either adherent to the ECM, localized on cell surfaces, or found in small secretory vesicles [44]. In our system, we added AlgSulf via nutritive media. AlgSulf tend to bind and anchor to Matrigel which alters the mode of presentation of these polysaccharides to cells. Added at higher concentration compared to media supplements, it is possible that AlgSulf sequester the supplemented GF and decrease the rate of cell proliferation. However, the non-significant differences in insulin and EGF binding between sulfated and non-sulfated polysaccharides indicate that this is unlikely the main route of action. The QCM-D analysis reveals that AlgSulf resembling anchored GAGs do not bind to EGF nor insulin. On the other hand, ELISA results show that $AlgSulf_{2.0}$ presented in a soluble form, resembling soluble GAGs, do bind partially to EGF, however this binding to EGF is not significantly different from $AlgSulf_{0.0}$ and does not alone justify the selective inhibition noted against the tumorigenic T4–2 cells grown in EGF free condition. The same results of ELISA were noted at higher concentrations of AlgSulf (data not shown). It is worth noting that in the coculture system, S1 cells were EGF deprived a couple of days before adding the T4–2 nodules, yet their growth rate was not affected by AlgSulf, thus the reduction in proliferation is unlikely due to EGF sequestration. Additionally, for parameter controlling purposes, AlgSulf-treated S1 and T4–2 cells grown in GF-reduced Matrigel (used as a negative control) showed similar responses to AlgSulf treated S1 and T4–2 cells grown in GF-loaded Matrigel. However, AlgSulf treated MDA-MB-231 supplemented with 10% serum showed an attenuated response to AlgSulf compared to serum starved cells. Obtaining significant responses in 10% serum cultures required a higher concentration of AlgSulf (data not shown). Thus, *in vivo* studies in the future are needed to confirm our results and elucidate the herein observed responses.

Our previous studies have shown that AlgSulf, especially with intermediate DS, has high affinity to HN-binding GFs such as FGF-2, NGF and IGF through ELISA and/or QCM-D analysis [20,21,23]. For example, the binding of AlgSulf to FGF-2 controls stem cells [21] and neural cell lines [20]. In addition, its binding to NGF enhances the viability of primary neurons and their neuronal network branching in 3D structures [23]. Moreover, AlgSulf modulates RhoA GTPase activity and Cyclin D1 gene expression in chondrocytes [29] and attenuates the expression of cancer stem cell/progenitor markers in KRAS-mutant lung cancer cells grown in 3D such as *ALDH1A1*, *CCL20*, *ALDH3A, Ccl20* and *Tnf* genes [24]. As such, any intervention in these pathways in breast cancer cells will ultimately result in affecting cell proliferation, differentiation, polarity, invasion and/or reversion.

A possible mechanism of AlgSulf induced antiproliferative effects and reversion of T4–2 nodules is sequestering GF other than EGF and insulin released by mammary epithelial cells that possess HN-binding domains rendering them unavailable to bind to GF receptors [70]. Another proposed mechanism of AlgSulf-induced growth arrest and reversion could be via blocking EGFR. Highly sulfated GAGs interact directly or indirectly with EGFR and modulate its pathways. For example, Decorin binding to EGFR in mammary carcinoma leads to receptor internalization, degradation, and subsequent shutting down of the downstream EGFR pathway; this has been significantly correlated with the elimination of tumor growth and metastasis [71]. Also, HN and HN species are reported to inhibit the activity of heparanase in head and neck carcinoma. Heparanase, a heparan cleavage enzyme, is strongly implicated in tumor metastasis attributed to activating EGFR through phosphorylation and activation of the downstream STAT3 pathway [72]. The reversion of T4–2 nodules is unlikely through the β1-integrin pathway as most sulfated GAGs promote cell-ECM interaction, cell adhesion, proliferation, and migration through directly binding and activating integrin receptors without inhibiting it, to the best of our knowledge (reviewed in [73,74]).

While we have not performed any binding/interaction assessment of our exogenous sulfated polysaccharides to intrinsic GAGs, in principle, our soluble AlgSulf can bind and affect the functionality of GAGs in the ECM. Like HN [75] and other sulfated GAGs supplemented exogenously, we do expect an interplay between AlgSulf and GAG-related signaling complexes to modulate cancer cell adhesion, chemotaxis, and migration.

In conclusion, we demonstrate that biomimetic sulfated alginates selectively target proliferating tumorigenic breast cells without disrupting the polarity axis nor lumen assembly ability of nontumorigenic breast cells. In addition, biomimetic sulfated alginates significantly decrease the invasion potential and contribute to restoring cell polarization and lumen assembly to a limited population in the tumorigenic breast cells. Most sulfated GAGs are heterogeneous and inconsistent in their chemical composition, however, AlgSulf can be synthesized with controlled DS in large batches making it a promising molecule for systematic studies on the effect of GAG sulfation on tumor development, progression and effective therapies.

Declaration of Competing Interest

The authors declare that they have no known competing financial interests or personal relationships that could have appeared to influence the work reported in this paper.

Acknowledgments

The authors would like to acknowledge the support of the American University of Beirut Collaborative Research Stimulus (CRS) grant and the Lebanese National Council for Scientific Research (CNRS-L). Rabih Talhouk and Nataly Naser Al Deen are members of the International Breast Cancer and Nutrition (IBCN) project at Purdue University. Zeina Habli and Nataly Naser Al Deen are recipients of the AUB-CNRS-L Scholarship.

Supplementary materials

Supplementary material associated with this article can be found, in the online version, at doi:10.1016/j.actbio.2020.12.049.

References

[1] J. Ferlay, I. Soerjomataram, R. Dikshit, S. Eser, C. Mathers, M. Rebelo, D.M. Parkin, D. Forman, F. Bray, Cancer incidence and mortality worldwide: sources, methods and major patterns in GLOBOCAN 2012, Int. J. Cancer 136 (5) (2015) E359–E386.

[2] A. Ahmad, in: Breast Cancer statistics: Recent trends, Breast Cancer Metastasis and Drug Resistance, Springer, 2019, pp. 1–7.

[3] J. Insua-Rodríguez, T. Oskarsson, The extracellular matrix in breast cancer, Adv. Drug Deliv. Rev. 97 (2016) 41–55.

[4] C.I. Gama, S.E. Tully, N. Sotogaku, P.M. Clark, M. Rawat, N. Vaidehi, W.A. Goddard 3rd, A. Nishi, L.C. Hsieh-Wilson, Sulfation patterns of glycosaminoglycans encode molecular recognition and activity, Nat. Chem. Biol. 2 (9) (2006) 467–473.

[5] M. Kusche-Gullberg, L. Kjellén, Sulfotransferases in glycosaminoglycan biosynthesis, Curr. Opin. Struct. Biol. 13 (5) (2003) 605–611.

[6] F. Grandoni, L. Alberio, Direct oral anticoagulant drugs: on the treatment of cancer-related venous thromboembolism and their potential anti-neoplastic effect, Cancers (Basel) 11 (1) (2019) 46.
[7] L. Borsig, R. Wong, J. Feramisco, D.R. Nadeau, N.M. Varki, A. Varki, Heparin and cancer revisited: mechanistic connections involving platelets, P-selectin, carcinoma mucins, and tumor metastasis, Proc. Natl. Acad. Sci. 98 (6) (2001) 3352–3357.
[8] J.-P. Li, Heparin, heparan sulfate and heparanase in cancer: remedy for metastasis? Anti-Cancer Agents Med. Chem. 8 (1) (2008) 64–76.
[9] F. Robert, The potential benefits of low-molecular-weight heparins in cancer patients, J. Hematol. Oncol. 3 (1) (2010) 3.
[10] G.R. Santos, A.M. Tovar, N.V. Capillé, M.S. Pereira, V.H. Pomin, P.A. Mourão, Structural and functional analyses of bovine and porcine intestinal heparins confirm they are different drugs, Drug Discov. Today 19 (11) (2014) 1801–1807.
[11] K. Ishida, M.K. Wierzba, T. Teruya, S. Simizu, H. Osada, Novel heparan sulfate mimetic compounds as antitumor agents, Chem. Biol. 11 (3) (2004) 367–377.
[12] C.Y. Pumphrey, A.M. Theus, S. Li, R.S. Parrish, R.D. Sanderson, Neoglycans, carbodiimide-modified glycosaminoglycans: a new class of anticancer agents that inhibit cancer cell proliferation and induce apoptosis, Cancer Res. 62 (13) (2002) 3722–3728.
[13] C.C. Reed, A. Waterhouse, S. Kirby, P. Kay, R.T. Owens, D.J. McQuillan, R.V. Iozzo, Decorin prevents metastatic spreading of breast cancer, Oncogene 24 (6) (2005) 1104–1110.
[14] Y. Xu, K. Chandarajoti, X. Zhang, V. Pagadala, W. Dou, D.M. Hoppensteadt, E.M. Sparkenbaugh, B. Cooley, S. Daily, N.S. Key, D. Severynse-Stevens, J. Fareed, R.J. Linhardt, R. Pawlinski, J. Liu, Synthetic oligosaccharides can replace animal-sourced low-molecular weight heparins, Sci. Transl. Med. 9 (406) (2017).
[15] C.I. Gama, L.C. Hsieh-Wilson, Chemical approaches to deciphering the glycosaminoglycan code, Curr. Opin. Chem. Biol. 9 (6) (2005) 609–619.
[16] L.L. Kiessling, J.C. Grim, Glycopolymer probes of signal transduction, Chem. Soc. Rev. 42 (10) (2013) 4476–4491.
[17] R.A. Scott, A. Panitch, Glycosaminoglycans in biomedicine, Wiley Interdisc. Rev. 5 (4) (2013) 388–398.
[18] N.L. Francis, M.S. Shanbhag, I. Fischer, M.A. Wheatley, Influence of alginate cross-linking method on neurite response to microencapsulated neurotrophin-producing fibroblasts, J. Microencapsul. 28 (5) (2011) 353–362.
[19] J. Sun, H. Tan, Alginate-based biomaterials for regenerative medicine applications, Materials (Basel) 6 (4) (2013) 1285–1309.
[20] W. Malaeb, H.F. Bahmad, W. Abou-Kheir, R. Mhanna, The sulfation of biomimetic glycosaminoglycan substrates controls binding of growth factors and subsequent neural and glial cell growth, Biomater. Sci. 7 (10) (2019) 4283–4298.
[21] R. Mhanna, J. Becher, M. Schnabelrauch, R.L. Reis, I. Pashkuleva, Sulfated alginate as a mimic of sulfated glycosaminoglycans: binding of growth factors and effect on stem cell behavior, Adv. Biosyst. 1 (7) (2017) 1700043.
[22] I. Freeman, A. Kedem, S. Cohen, The effect of sulfation of alginate hydrogels on the specific binding and controlled release of heparin-binding proteins, Biomaterials 29 (22) (2008) 3260–3268.
[23] G. Kfoury, V.El Habbaki, W. Malaeb, S. Weaver, D. Momotenko, R. Mhanna, Alginate Sulfate Substrates Control Growth Factor Binding and Growth of Primary Neurons: toward Engineered 3D Neural Networks, Adv. Biosyst. (2020) 2000047.
[24] N. Al Matari, G. Deeb, H. Mshiek, A. Sinjab, H. Kadara, W. Abou-Kheir, R. Mhanna, Anti-Tumor Effects of Biomimetic Sulfated Glycosaminoglycans on Lung Adenocarcinoma Cells in 2D and 3D In Vitro Models, Molecules 25 (11) (2020) 2595.
[25] P. Briand, O. Petersen, B. Van Deurs, A new diploid nontumorigenic human breast epithelial cell line isolated and propagated in chemically defined medium, *In vitro* cellular & dev. Biol. 23 (3) (1987) 181–188.
[26] P. Briand, K.V. Nielsen, M.W. Madsen, O.W. Petersen, Trisomy 7p and malignant transformation of human breast epithelial cells following epidermal growth factor withdrawal, Cancer Res. 56 (9) (1996) 2039–2044.
[27] C. Plachot, S.A. Lelièvre, DNA methylation control of tissue polarity and cellular differentiation in the mammary epithelium, Exp. Cell Res. 298 (1) (2004) 122–132.
[28] P.-A. Vidi, M.J. Bissell, S.A. Lelièvre, Three-dimensional culture of human breast epithelial cells: the how and the why, in: Epithelial Cell Culture Protocols, Springer, 2012, pp. 193–219.
[29] R. Mhanna, A. Kashyap, G. Palazzolo, Q. Vallmajo-Martin, J. Becher, S. Möller, M. Schnabelrauch, M. Zenobi-Wong, Chondrocyte culture in three dimensional alginate sulfate hydrogels promotes proliferation while maintaining expression of chondrogenic markers, Tissue Eng. Part A 20 (9–10) (2014) 1454–1464.
[30] M. Zenobi-Wong, G. Palazzolo, R. Mhanna, J. Becher, S. Moller, M. Schnabelrauch, Sulfated Alginate Hydrogels For Cell Culture and Therapy, Google Patents, 2018.
[31] H. Ronghua, D. Yumin, Y. Jianhong, Preparation and *in vitro* anticoagulant activities of alginate sulfate and its quaterized derivatives, Carbohydr. Polym. 52 (1) (2003) 19–24.
[32] Ø. Arlov, F.L. Aachmann, A. Sundan, T. Espevik, G. Skjåk-Bræk, Heparin-like properties of sulfated alginates with defined sequences and sulfation degrees, Biomacromolecules 15 (7) (2014) 2744–2750.
[33] V. Hintze, A. Miron, S. Moeller, M. Schnabelrauch, H.P. Wiesmann, H. Worch, D. Scharnweber, Sulfated hyaluronan and chondroitin sulfate derivatives interact differently with human transforming growth factor-β1 (TGF-β1), Acta Biomater. 8 (6) (2012) 2144–2152.
[34] R.J. Blaschke, A.R. Howlett, P.-Y. Desprez, O.W. Petersen, M.J. Bissell, [25]Cell differentiation by extracellular matrix components, in: Methods in Enzymology, Elsevier, 1994, pp. 535–556.
[35] S. Fostok, M. El-Sibai, D. Bazzoun, S. Lelièvre, R. Talhouk, Connexin 43 loss triggers cell cycle entry and invasion in non-neoplastic breast epithelium: a role for noncanonical wnt signaling, Cancers (Basel) 11 (3) (2019) 339.
[36] E. Nilebäck, L. Feuz, H. Uddenberg, R. Valiokas, S. Svedhem, Characterization and application of a surface modification designed for QCM-D studies of biotinylated biomolecules, Biosens. Bioelectron. 28 (1) (2011) 407–413.
[37] D. Bazzoun, H. Adissu, L. Wang, A. Urazaev, I. Tenvooren, S. Fostok, S. Chittiboyina, J. Sturgis, K. Hodges, G. Chandramouly, Connexin 43 maintains tissue polarity and regulates mitotic spindle orientation in the breast epithelium, J. Cell. Sci. 132 (10) (2019) jcs223313.
[38] A. Chhetri, S. Chittiboyina, F. Atrian, Y. Bai, D.A. Delisi, R. Rahimi, J. Garner, Y. Efremov, K. Park, R. Talhouk, Cell Culture and Coculture for Oncological Research in Appropriate Microenvironments, Curr. Protoc. Chem. Biol. 11 (2) (2019) e65.
[39] P.A. Vidi, T. Maleki, M. Ochoa, L. Wang, S.M. Clark, J.F. Leary, S.A. Lelièvre, Disease-on-a-chip: mimicry of tumor growth in mammary ducts, Lab Chip 14 (1) (2014) 172–177.
[40] F. Wang, R.K. Hansen, D. Radisky, T. Yoneda, M.H. Barcellos-Hoff, O.W. Petersen, E.A. Turley, M.J. Bissell, Phenotypic reversion or death of cancer cells by altering signaling pathways in three-dimensional contexts, J. Natl. Cancer Inst. 94 (19) (2002) 1494–1503.
[41] V.M. Weaver, O.W. Petersen, F. Wang, C. Larabell, P. Briand, C. Damsky, M.J. Bissell, Reversion of the malignant phenotype of human breast cells in three-dimensional culture and *in vivo* by integrin blocking antibodies, J. Cell Biol. 137 (1) (1997) 231–245.
[42] P.A. Kenny, M.J. Bissell, Tumor reversion: correction of malignant behavior by microenvironmental cues, Int. J. Cancer 107 (5) (2003) 688–695.
[43] B.L. Ricca, G. Venugopalan, S. Furuta, K. Tanner, W.A. Orellana, C.D. Reber, D.G. Brownfield, M.J. Bissell, D.A. Fletcher, Transient external force induces phenotypic reversion of malignant epithelial structures via nitric oxide signaling, Elife 7 (2018) e26161.
[44] N. Afratis, C. Gialeli, D. Nikitovic, T. Tsegenidis, E. Karousou, A.D. Theocharis, M.S. Pavão, G.N. Tzanakakis, N.K. Karamanos, Glycosaminoglycans: key players in cancer cell biology and treatment, FEBS J. 279 (7) (2012) 1177–1197.
[45] L. Kjellén, U. Lindahl, Specificity of glycosaminoglycan–protein interactions, Curr. Opin. Struct. Biol. 50 (2018) 101–108.
[46] V.N. Patel, D.L. Pineda, M.P. Hoffman, The function of heparan sulfate during branching morphogenesis, Matrix Biol. 57 (2017) 311–323.
[47] J. Umbreit, Proteoglycans and glycosaminoglycans during maturation of the mouse mammary gland, Anticancer Res. 16 (5A) (1996) 3013–3029.
[48] M. Fujii, A. Yusa, Y. Yokoyama, T. Kokuryo, N. Tsunoda, K. Oda, M. Nagino, T. Ishimaru, Y. Shimoyama, H. Utsunomiya, Cytoplasmic expression of the JM403 antigen GlcA-GlcNH 3+ on heparan sulfate glycosaminoglycan in mammary carcinomas—A novel proliferative biomarker for breast cancers with high malignancy, Glycoconj. J. 27 (7–9) (2010) 661–672.
[49] A. Pudełko, G. Wisowski, K. Olczyk, E.M. Koźma, The dual role of the glycosaminoglycan chondroitin-6-sulfate in the development, progression and metastasis of cancer, FEBS J. 286 (10) (2019) 1815–1837.
[50] L. Fan, L. Jiang, Y. Xu, Y. Zhou, Y. Shen, W. Xie, Z. Long, J. Zhou, Synthesis and anticoagulant activity of sodium alginate sulfates, Carbohydr. Polym. 83 (4) (2011) 1797–1803.
[51] R. Mhanna, Engineering Chondrogenic Micro-Environments For Tissue Engineering Applications, ETH Zurich, 2013.
[52] R.K. Okolicsanyi, M. Faure, J.M. Jacinto, D. Chacon-Cortes, S. Chambers, P.H. Youl, L.M. Haupt, L.R. Griffiths, Association of the SNP rs2623047 in the HSPG modification enzyme SULF1 with an Australian Caucasian breast cancer cohort, Gene 547 (1) (2014) 50–54.
[53] U. Nilsson, R. Johnsson, L.-Å. Fransson, U. Ellervik, K. Mani, Attenuation of tumor growth by formation of antiproliferative glycosaminoglycans correlates with low acetylation of histone H3, Cancer Res. 70 (9) (2010) 3771–3779.
[54] A. Nyga, U. Cheema, M. Loizidou, 3D tumour models: novel *in vitro* approaches to cancer studies, J. Cell Commun. Signal 5 (3) (2011) 239.
[55] P. Kenny, Three-dimensional Extracellular Matrix Culture Models of EGFR Signalling and Drug Response, Portland Press Ltd., 2007.
[56] A. Riedl, M. Schlederer, K. Pudelko, M. Stadler, S. Walter, D. Unterleuthner, C. Unger, N. Kramer, M. Hengstschläger, L. Kenner, Comparison of cancer cells in 2D *vs* 3D culture reveals differences in AKT–mTOR–S6K signaling and drug responses, J. Cell Sci. 130 (1) (2017) 203–218.
[57] S.J. Chatterjee, L. McCaffrey, Emerging role of cell polarity proteins in breast cancer progression and metastasis, Breast Cancer 6 (2014) 15.
[58] G. Chandramouly, P.C. Abad, D.W. Knowles, S.A. Lelièvre, The control of tissue architecture over nuclear organization is crucial for epithelial cell fate, J. Cell. Sci. 120 (9) (2007) 1596–1606.
[59] S.A. Lelièvre, Tissue polarity-dependent control of mammary epithelial homeostasis and cancer development: an epigenetic perspective, J. Mammary Gland Biol. Neoplasia 15 (1) (2010) 49–63.
[60] L. Dow, J. Kauffman, J. Caddy, A. Peterson, S. Jane, S. Russell, P. Humbert, The tumour-suppressor Scribble dictates cell polarity during directed epithelial migration: regulation of Rho GTPase recruitment to the leading edge, Oncogene 26 (16) (2007) 2272–2282.
[61] P. Astudillo, H. Carrasco, J. Larraín, Syndecan-4 inhibits Wnt/β-catenin signaling through regulation of low-density-lipoprotein receptor-related protein (LRP6) and R-spondin 3, Int. J. Biochem. Cell Biol. 46 (2014) 103–112.

[62] C.M. Willis, M. Klüppel, Chondroitin sulfate-E is a negative regulator of a pro–tumorigenic Wnt/beta-catenin-Collagen 1 axis in breast cancer cells, PLoS ONE 9 (8) (2014).
[63] A. Rizki, V.M. Weaver, S.-Y. Lee, G.I. Rozenberg, K. Chin, C.A. Myers, J.L. Bascom, J.D. Mott, J.R. Semeiks, L.R. Grate, A human breast cell model of preinvasive to invasive transition, Cancer Res. 68 (5) (2008) 1378–1387.
[64] B. Weigelt, C.M. Ghajar, M.J. Bissell, The need for complex 3D culture models to unravel novel pathways and identify accurate biomarkers in breast cancer, Adv. Drug Deliv. Rev. 69-70 (2014) 42–51.
[65] P.A. Kenny, G.Y. Lee, C.A. Myers, R.M. Neve, J.R. Semeiks, P.T. Spellman, K. Lorenz, E.H. Lee, M.H. Barcellos-Hoff, O.W. Petersen, J.W. Gray, M.J. Bissell, The morphologies of breast cancer cell lines in three-dimensional assays correlate with their profiles of gene expression, Mol. Oncol. 1 (1) (2007) 84–96.
[66] N. Tasdemir, E.A. Bossart, Z. Li, L. Zhu, M.J. Sikora, K.M. Levine, B.M. Jacobsen, G.C. Tseng, N.E. Davidson, S. Oesterreich, Comprehensive Phenotypic Characterization of Human Invasive Lobular Carcinoma Cell Lines in 2D and 3D Cultures, Cancer Res. 78 (21) (2018) 6209–6222.
[67] D.P. Saraiva, A.T. Matias, S. Braga, A. Jacinto, M.G. Cabral, Establishment of a 3D Co-culture With MDA-MB-231 Breast Cancer Cell Line and Patient-Derived Immune Cells for Application in the Development of Immunotherapies, Front Oncol. 10 (2020) 1543.
[68] A. Weltrowski, M.-.L. da Silva Almeida, D. Peschel, K. Zhang, S. Fischer, T. Groth, Mitogenic Activity of Sulfated Chitosan and Cellulose Derivatives is Related to Protection of FGF-2 from Proteolytic Cleavage, Macromol. Biosci. 12 (6) (2012) 740–750.
[69] D. Peschel, K. Zhang, S. Fischer, T. Groth, Modulation of osteogenic activity of BMP-2 by cellulose and chitosan derivatives, Acta Biomater. 8 (1) (2012) 183–193.
[70] B.A. Thorne, G.D. Plowman, The heparin-binding domain of amphiregulin necessitates the precursor pro-region for growth factor secretion, Mol. Cell. Biol. 14 (3) (1994) 1635–1646.
[71] M. Santra, I. Eichstetter, R.V. Iozzo, An anti-oncogenic role for decorin Down-regulation of ErbB2 leads to growth suppression and cytodifferentiation of mammary carcinoma cells, J. Bio. Chem. 275 (45) (2000) 35153–35161.
[72] V. Cohen-Kaplan, I. Doweck, I. Naroditsky, I. Vlodavsky, N. Ilan, Heparanase augments epidermal growth factor receptor phosphorylation: correlation with head and neck tumor progression, Cancer Res. 68 (24) (2008) 10077–10085.
[73] S. Ricard-Blum, Protein–glycosaminoglycan interaction networks: focus on heparan sulfate, Perspectives Sci. 11 (2017) 62–69.
[74] D. Nikitovic, K. Kouvidi, K. Voudouri, A. Berdiaki, E. Karousou, A. Passi, G.N. Tzanakakis, The motile breast cancer phenotype roles of proteoglycans/glycosaminoglycans, Biomed. Res. Int. (2014) 2014.
[75] P. Mellor, J.R. Harvey, K.J. Murphy, D. Pye, G. O'Boyle, T.W.J. Lennard, J.A. Kirby, S. Ali, Modulatory effects of heparin and short-length oligosaccharides of heparin on the metastasis and growth of LMD MDA-MB 231 breast cancer cells *in vivo*, Br. J. Cancer 97 (6) (2007) 761–768.